

Vision Foundation Models in Agriculture: Toward Domain-Specific Adaptation for Weed Herbicide Trials Assessment

Leire Benito-Del-Valle^{a,b,*}, Artzai Picón^{a,b}, Daniel Mugica^a, Manuel Ramos^{c,b}, Eva Portillo^b, Javier Romero^d, Carlos Javier Jimenez^d, Ramón Navarra-Mestre^e

^aTECNALIA, Basque Research and Technology Alliance (BRTA), Parque Tecnológico de Bizkaia, C/ Geldo. Edificio 700, E-48160 Derio - Bizkaia (Spain)

^bUniversity of the Basque Country, Plaza Torres Quevedo, 48013 Bilbao (Spain)

^cBASF Digital Solutions S.L, Camino Fuente de la Mora 1, 28050 Madrid (Spain)

^dBASF Espanola S.L. Carretera A376, 41710 Utrera, Sevilla (Spain)

^eBASF SE, Speyererstrasse 2, 67117 Limburgerhof (Germany)

Abstract

Herbicide field trials require accurate identification of plant species and assessment of herbicide-induced damage across diverse environments. While general-purpose vision foundation models have shown promising results in complex visual domains, their performance can be limited in agriculture, where fine-grained distinctions between species and damage types are critical.

In this work, we adapt a general-purpose vision foundation model to herbicide trial characterization. Trained using a self-supervised learning approach on a large, curated agricultural dataset, the model learns rich and transferable representations optimized for herbicide trials images.

Our domain-specific model significantly outperforms the best general-purpose foundation model in both species identification (F1 score improvement from 0.91 to 0.94) and damage classification (from 0.26 to 0.33). Under unseen conditions (new locations and other time), it achieves even greater gains (species identification from 0.56 to 0.66; damage classification from 0.17 to 0.27). In domain-shift scenarios, such as drone imagery, it maintains strong performance (species classification from 0.49 to 0.60).

Additionally, we show that domain-specific pretraining enhances segmentation accuracy, particularly in low-annotation regimes. An annotation-efficiency analysis reveals that, under unseen conditions, the domain-specific model achieves 5.4% higher F1 score than the general-purpose model, while using 80% fewer labeled samples.

These results demonstrate the generalization capabilities of domain-specific foundation models and their potential to significantly reduce manual annotation efforts, offering a scalable and automated solution for herbicide trial analysis.

Keywords: Foundation Models, Large Visual Models, Plant Species and Damage segmentation, Precision Agriculture, Precise Phenotyping

1. Introduction

Weed management is a critical challenge in modern agriculture, directly impacting crop yields, food security, and economic sustainability (Kumar et al. (2024)). Weeds compete with crops for essential resources like soil,

*Corresponding author at: TECNALIA, Basque Research and Technology Alliance (BRTA), Parque Tecnológico de Bizkaia, C/ Geldo. Edificio 700, E-48160 Derio- Bizkaia, Spain

Email address: leire.benitodelvalle@tecnalia.com (Leire Benito-Del-Valle)

nutrients and sunlight, ultimately slowing growth and reducing yields. Moreover, many weed species serve as hosts for pests and pathogens, further compromising crop health.

To manage weed populations and optimize crop yield, traditional weed management methods are commonly employed, such as manual removal or broad-spectrum herbicide application. These methods, however, are labor-intensive, costly and environmentally unsustainable (Oerke (2006)). Thus, accurate weed detection and segmentation in crops are essential for precision agriculture, enabling targeted interventions that minimize herbicide use and reduce environmental impact. Automated weed detection systems, utilizing technologies such as deep learning and computer vision ease the identification and management of weeds, reducing reliance on manual labor (Hu et al. (2024)). Furthermore, precision spraying technologies can reduce herbicide usage, thereby diminishing environmental contamination (Darbyshire et al. (2023)).

Initially, machine learning (ML) approaches have been employed to classify or detect crops and weeds, relying on manual feature engineering techniques such as texture and color histograms (Juwono et al. (2023)). These methods often lack generalizability across varying field conditions and crop types due to their dependence on handcrafted features (Adhinata et al. (2024)). Therefore, the introduction of deep learning (DL) has marked a turning point, enabling end-to-end learning from raw imagery and significantly improving performance in all tasks.

Mortensen et al. (2016) first applied deep learning to crop and weed semantic segmentation, achieving 79% pixel accuracy for plant species. They later improved the method, enabling the discernment of corn from 23 weed species with a 94% pixel-wise accuracy (Dyrmann et al. (2016)).

However, like many DL-based methods, these approaches heavily rely on large, manually annotated datasets. When developing effective weed detection systems, large, diverse, and accurately annotated datasets are needed to train precise deep learning algorithms. Acquiring such datasets, however, is time-consuming, costly and often impractical. For instance, the progression of diseases and weed growth in natural environments is prone to significant changes, making it hard to capture a large variability. Consequently, these models tend to perform poorly in the underrepresented regions or require mayor redesign to incorporate novel weed species.

To reduce the burden of manual labeling, various strategies have been proposed. Bosilj et al. (2020) have shown that transfer learning can significantly reduce annotation demands while maintaining high accuracy in crop and weed discrimination. Other approaches have focused on architectural improvements, such as weedNet (Sa et al. (2018)), which achieves an 80% F1 score using an encoder-decoder cascaded deep neural network (Segnet), and Milioto et al. (2018), who integrate task-relevant background knowledge into the network to improve generalization and real-time inference performance. Similarly, Ma et al. (2019) employ a fully convolutional network for rice and weed segmentation, reporting an average accuracy of 92.7%.

Another setback when developing effective weed detection systems is distinguishing weeds from crops. This is primarily due to the fine-grained visual similarities between weeds and crops, especially during early growth stages, as well as the significant intra-class variability among weed species. To overcome this, probabilistic methods have been suggested for uncertainty estimation (Celikkan et al. (2023)).

These prior approaches have targeted the identification and segmentation of healthy plants. While this is effective for precision agriculture applications, it does not fully address the needs of automating herbicide research and development. In these field trials, it is necessary to not only distinguish between healthy plant species, but also to segment damaged plants and quantify different types of damage for each species. This adds further complexity to the problem.

Given the fine-grained nature of plant species identification, recent research has explored how incorporating taxonomic relationships among species can enhance model performance. Picon et al. (2025b) propose a hierarchical loss function for semantic segmentation tasks that leverages taxonomic relationships between species, plant damages, and other related factors, allowing models to benefit from partially annotated data.

While this approach has demonstrated strong performance in field trials, effectively addressing key challenges in crop-weed discrimination and damage quantification, its evaluation has been limited to in-domain data. As a result, its ability to generalize to unseen conditions remains unclear. This limitation restricts its applicability in real-world scenarios, where environmental variability and species diversity are prevalent.

Recently, foundation models have emerged, which address the growing demand for large-scale datasets. These models are trained on vast amounts of data and are capable of producing representations that can be applied across a wide range of tasks and domains (Bommasani et al. (2022)). A particularly promising approach involves training foundation models using self-supervised learning (SSL), which is especially useful in areas like agriculture where publicly available image data is scarce. SSL works by altering data in a way that creates implicit labels, allowing models to learn without explicit annotations.

A notable example is DINOv2 (Oquab et al. (2024)), a vision foundation model trained using SSL techniques that learns robust and transferable visual features without supervision. DINOv2 has shown strong performance across various downstream tasks, and has shown great potential in agriculture. Picon et al. (2025a) applied DINOv2 for weed and damage segmentation in herbicide trials, demonstrating its robustness under domain shifts. Similarly, Espejo-Garcia et al. (2025) evaluated DINOv2’s adaptability across multiple agricultural datasets, highlighting its effectiveness in disease detection, weed identification, and growth stage classification, even with minimal fine-tuning.

Building on this, DINOv3 (Siméoni et al. (2025)) introduces further improvements by scaling both the data and the model size, and by incorporating novel techniques such as Gram anchoring. It (DINOv3_web) achieves state-of-the-art results across diverse vision tasks without fine-tuning and introduces variants tailored for satellite imagery (DINOv3_sat), showcasing the potential of domain-specific adaptations.

Despite these advancements, most large vision foundation models remain general-purpose and are not adapted to specialized domains like agriculture. In particular, herbicide trials present unique challenges, such as high intra-species variability and the need for fine-grained damage assessment, that continue to pose difficulties for existing models. Building on these observations, we propose that domain-specific adaptations, particularly those leveraging self-supervised learning, could lead to significant performance improvements in real-world agricultural settings.

The goal of this work is to develop a domain-specific large vision foundation model for herbicide trials, using a self-supervised learning approach. By tailoring the model to agricultural imagery, we aim to reduce the need for annotated data and improve generalization across diverse real-world conditions.

The main contributions are as follows:

- A domain-specific vision foundation model for herbicide trials, is proposed. It is trained using a self-supervised learning approach on a large curated dataset, enabling the model to learn rich and transferable representations tailored to agricultural imagery.
- A comparative evaluation is performed against state-of-the-art general-purpose foundation models on multi-

species and damage plant semantic segmentation tasks. This comparison highlights the benefits of domain-specific pretraining for agricultural applications.

- The robustness of the model is evaluated under domain shifts, including changes in camera types, geographic locations, and capture protocols, confirming its generalization capabilities in real-world agricultural scenarios.
- A detailed annotation-efficiency analysis is performed. By gradually decreasing the amount of labeled training data, we assess the model’s performance in low-annotation regimes and its potential to reduce reliance on manual labeling.

2. Materials

In this section, we describe the datasets employed for the generation and evaluation of the domain-specific foundation model. Each dataset serves a distinct purpose in the training and evaluation pipeline (see Section 3 for a detailed explanation of the pipeline):

- Herbicide trials dataset: used to train the domain-specific foundation model through self-supervised learning.
- Primitives dataset: employed to monitor learning progress during self-supervised pretraining.
- Base dataset: used for supervised fine-tuning of segmentation decoders and performance evaluation.
- Reality check dataset: applied to assess model generalization capabilities under temporal and environmental domain shifts.
- Reality check DRONE dataset: used to evaluate model robustness under extreme domain shifts involving different sensor modalities and capture protocols.

2.1. *Herbicides trials dataset*

To develop a domain-specific foundation model, it is essential to gather a large and well-curated dataset. For this purpose, we compiled all available herbicide trial images (BASF Agricultural Solutions), resulting in an initial dataset comprising 340,554 images. These were acquired using diverse sensors across multiple geographic locations, years, and crop types, ensuring substantial diversity in environmental conditions and visual characteristics.

Although the dataset offers broad variability, its quality cannot be guaranteed without further inspection. Therefore, an initial data curation step was performed to identify and remove low-quality samples. Specifically, blurry images, exact duplicates, near-duplicates, and excessively dark samples were discarded, reducing the dataset to 261,891 images.

From these curated images, we generated non-overlapping tiles of 518x518 pixels, yielding a total of 11.8M image patches. The large number of tiles is attributed to the high resolution and extensive field coverage of the original images, which often contain multiple crop rows and treatment zones.

Following tiling, we observed substantial variation in vegetation coverage across the dataset. To ensure that the model learns meaningful representations of vegetation presence and structure, rather than relying on superficial cues such as dominant color or background texture, we performed a balancing step based on vegetation content. Using segmentation masks generated by an existing vegetation segmentation model, we computed the percentage

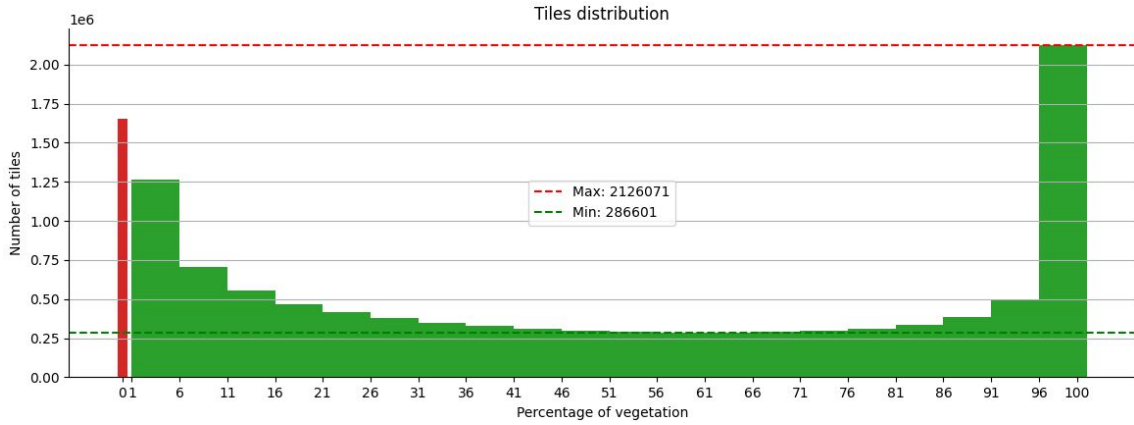


Figure 1: Distribution of image tiles based on vegetation coverage.

of vegetation present in each tile. The distribution of vegetation coverage is shown in Figure 1, revealing a strong imbalance.

To address this, we used the predefined vegetation coverage intervals shown in Figure 1 and selected an equal number of tiles from each interval. This approach ensures a uniform representation of vegetation density across the dataset, promoting more robust and generalizable feature learning during model training.

After this final balancing step, we obtained a curated dataset of 6M image tiles (see Figure 2), which was used to train the domain-specific foundation model.



Figure 2: Image samples from the curated herbicides trials dataset.

2.2. Base dataset

For the Base dataset, we employed a reduced version of the dataset presented in Picon et al. (2025b), where a carefully compiled and manually annotated dataset was generated between 2018 and 2020. This dataset comprises a wide range of crop and weed species collected from real plot fields over multiple years. The 14 species included are: *Abutilon theophrasti* (eppo: ABUTH), *Amaranthus retroflexus* (eppo: AMARE), *Chenopodium album* (eppo: CHEAL), *Digitaria sanguinalis* (eppo: DIGSA), *Echinochloa crus-galli* (eppo: ECHCG), *Portulaca oleracea* (eppo: POROL), *Setaria viridis* (eppo: SETVE), *Datura stramonium* (eppo: DATST), *Echinochloa colona* (eppo: ECHCO), *Glycine max* (eppo: GLXMA), *Helianthus annuus* (eppo: HELAN), *Polygonum convolvulus* (eppo: POLCO), *Solanum nigrum* (eppo: SOLNI), and maize, *Zea mays* (eppo: ZEAMX).

The dataset features images depicting 6 types of plant damage, such as INITIAL, INITIAL-BLEACHING, INITIAL-NECROSIS, BLEACHING, NECROSIS, and LEAF-CURLING, along with annotated growth stages. These images were captured under diverse environmental conditions and locations. Moreover, two dataset formats were developed: type A, which contains real field images with multiple species, and type C, in which only individual species are present.

In this study, we focus exclusively on Type A datasets from 2019, representing a reduction of 82.48% in data size (from 2449 to 429). This choice aligns with our objective of minimizing the amount of labeled data required for effective model training.

Annotation was performed using CVAT (Sekachev et al. (2020)), and further refined using existing vegetation segmentation models. Metadata such as location and image field of view were included to support scale correction and data augmentation. All species are labeled using their respective EPPO codes (Ayllón-Benitez et al. (2023)).

Species abundance and distribution vary across plots due to environmental factors and species-specific traits, resulting in a rich diversity within the dataset. A detailed overview of the contents of the dataset is provided in Table 1.

Collection	Type	Images	Species	Damage	Location
2019A1	A	147	ABUTH, AMARE, CHEAL, DATST, DIGSA, ECHCG, ECHCO, GLXMA, HELAN, POLCO, POROL, SETVE, SOLNI, ZEAMX	INITIAL, INITIAL- BLEACHING, INITIAL-NECROSIS, BLEACHING, NECROSIS	ES, DE
2019A2	A	282	ABUTH, AMARE, CHEAL, DATST, DIGSA, ECHCG, ECHCO, GLXMA, HELAN, POLCO, POROL, SETVE, SOLNI, ZEAMX	INITIAL- BLEACHING, INITIAL-NECROSIS, BLEACHING, NECROSIS	ES, DE

Table 1: BASE dataset content summary.

An example of the annotated images is shown in Figure 3, which illustrates how species, and damage types are labeled. Given the inherent uncertainty in the annotation process, we introduced additional class labels to handle ambiguous cases. These include categories for unidentified broadleaf species (other-broad), unidentified grass species (other-grass), and instances where multiple species are present (other-mixed).

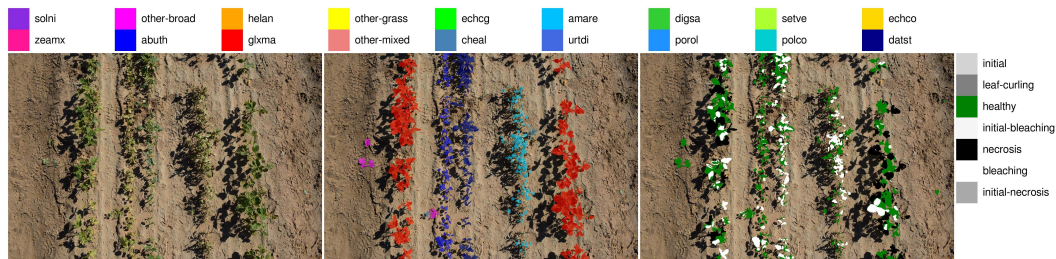


Figure 3: 2019A2 dataset. Example image with species, and damage masks. left) Original Image, middle) Species annotation, right) Damage annotation (Picon et al. (2025b)).

2.3. Primitives dataset

To evaluate the performance of the foundation model during training (SSL) and to select the optimal weights, we generated an auxiliary species classification dataset. This dataset is composed of primitives extracted from the original Base dataset described in Picon et al. (2025b). For this purpose, we exclusively used the C-type subsets,

as they contain images with a single species per image, ensuring consistency in labeling (Section 2.2). A detailed overview of the full images used for the primitive extraction is provided in Table 2.

The primitives dataset was constructed using the species semantic segmentation masks available at the image level. Each segmented blob was isolated to produce individual images representing distinct plant instances. Due to the simplicity of the cropping process, some primitives may contain overlapping plants. However, since all plants within a given image belong to the same species, this does not compromise the suitability of the dataset for classification tasks. An example of the primitives extracted from a single image is shown in Figure 4.

Collection	Type	Images	Species	Damage	Location
2019C1	C	249	ABUTH, AMARE, CHEAL, DATST, DIGSA, ECHCG, GLXMA, HELAN, POLCO, POROL, SETVE, SOLNI, ZEAMX	None	ES
2019C2	C	303	ABUTH, AMARE, CHEAL, DATST, DIGSA, ECHCG, GLXMA, HELAN, POLCO, POROL, SETVE, SOLNI, ZEAMX	NECROSIS	ES
2020CDE1	C	139	ABUTH, AMARE, CHEAL, DIGSA, ECHCG, POLCO, POROL	NECROSIS	DE
2020CES1	C	222	ABUTH, AMARE, CHEAL, DATST, DIGSA, ECHCG, ECHCO, GLXMA, HELAN, POLCO, POROL, SETVE, SOLNI	BLEACHING, NECROSIS, CURLING	ES

Table 2: BASE dataset content used to generate the primitives dataset.

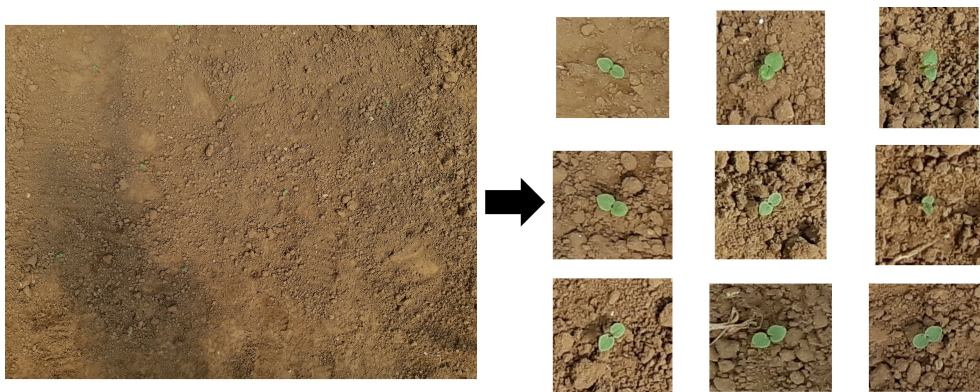


Figure 4: Primitive extraction example showing the original image (left) and the corresponding cropped regions (right) used as individual primitives.

2.4. Reality check (2023)

To assess the algorithm’s performance in unfamiliar scenarios, we utilized the same reality check dataset introduced in Picon et al. (2025a). This dataset was collected in 2023 across Germany, the United States, and

Spain. The images were acquired using mobile and digital cameras through the BASF crop digitalization app and annotated using CVAT (Sekachev et al. (2020)). It includes 35 identified crop and weed species, as well as broader categories for unidentified vegetation and species not present in the Base dataset (Section 2.2). These unclassified or novel species are grouped according to their botanical taxonomy into three categories: other-broad, other-grass, and other-mixed. Moreover, some species may not be present in this dataset due to environmental changes or other circumstances. A detailed overview of the contents of the dataset is provided in Table 3.

Collection	Type	Images	Species	Damage	Location
2023ADE	A	32	AMACH, CHEAL, DATST, ECHCG, GLXMA, HELAN, HORVX, LAMAM, LAMPU, LOLMU, MERAN, POLAM, POLCO, POLPE, POROL, SETVE, SETVI, SINAL, SPRAR, STEME, TRZAX, ZEAMX,	INITIAL, BLEACH-ING, NECROSIS, LEAF-CURLING	GERMANY
2023AES	A	36	AMABL, AMARE, CHEAL, DATST, DIGSA, ECHCG, GLXMA, HELAN, POLCO, POROL, SETVE, SETVI, SOLNI, ZEAMX,	INITIAL, NECROSIS, LEAF-CURLING	SPAIN
2023AUS	A	37	AMABL, AMAPA, AMARE, AM-ATU, CHEAL, CONAR, CYPES, DIGSA, ECHCG, ELEIN, GLXMA, HELAN, KCHSC, MOLVE, POLPY, POROL, SETPU, SETVI, ZEAMX,	INITIAL, BLEACH-ING, NECROSIS, LEAF-CURLING	UNITED STATES

Table 3: REALITY dataset content summary.

2.5. Reality check DRONE based dataset (2024)

To further evaluate the algorithm under conditions of significant data drift, we used the drone-based dataset introduced in Picon et al. (2025a). It was collected between late 2023 and 2024 in Spain, Germany, and the United States using DJI drones equipped with RGB sensors. The dataset includes images of maize (*Zea mays*, ZEAMX), sunflower (*Helianthus annuus*, HELAN), and soybean (*Glycine max*, GLXMA). A summary of the dataset is presented in Table 4.

Collection	Type	Images	Species	Damage	Location
UAV241122A		201	ABUTH, ACCOS, ALOMY, AMABL, AMACH, AMAPA, AMARE, AMATA, AMATU, ANGAR, AVEFA, BRSSN, CAPBP, CASOB, CHEAL, CHEHY, CIRAR, CONAR, CYPCP, CYPES, DATST, DIGSA, DTTAE, DTTSS, ECAEL, ECHCG, ECHCO, ELEIN, GALAP, GLXMA, GOSHI, HELAN, HISIN, HORVX, IPOHE, IPOLA, KCHSC, LAMAM, LAMPU, LOLMU, MERAN, MOLVE, OTHER-BROAD, OTHER-GRASS, OTHER-MIXED, PANDI, PANMI, PESGL, PIBSA, POLAM, POLCO, POLPE, POLPY, POROL, PORPI, RAPRA, RCHSC, SENVU, SETPU, SETVE, SETVI, SIDSP, SINAL, SOIL, SOLNI, SOLTU, SONOL, SORVU, SPRAR, STEME, TRBTE, TRZAX, URTDI, URTUR, VIOAR, ZEAMX	INITIAL, BLEACH-ING, NECROSIS, LEAF-CURLING	GERMANY, UNITED STATES, SPAIN,

Table 4: DRONE based reality dataset content summary.

3. Methods

This section introduces the methodology followed to obtain a domain-specific foundation model. The process is structured in two main stages (see Figure 5): self-supervised pretraining, in which the foundation model is formed by learning general domain representations from unlabeled data, and supervised fine-tuning, which serves to validate the model’s effectiveness on a downstream segmentation task.

3.1. Self-supervised pretraining

To obtain the domain-specific foundation model, we employed the large variant of DINOv2 with registers (ViT-L/14, 0.3B parameters)(Oquab et al. (2024)), a self-supervised learning framework based on vision transformers (ViT) (Dosovitskiy et al. (2021)). DINOv2 operates with a dual-network architecture, where a student network is trained to align with the output of a teacher network, whose weights are updated via an exponential moving average of the student. Images are split into patches and processed with a Vision Transformer backbone, followed by projection heads that produce feature representations. The training objective encourages the student to match the teacher’s output across augmented views, enabling stable self-supervised learning without labels.

The model was trained on the herbicides trials dataset (see Section 2.1) using the official DINOv2 implementation, starting from publicly available pretrained weights for the backbone. Since the DINOv2-specific heads are

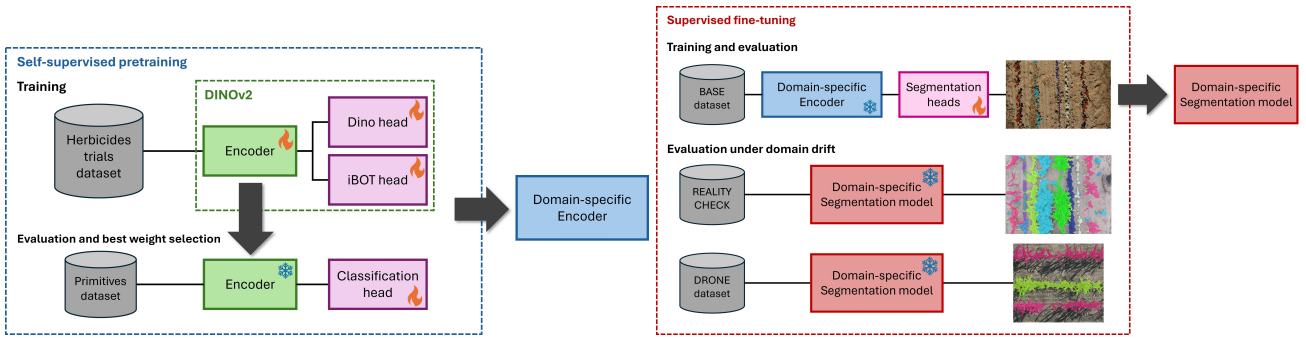


Figure 5: Overview of the proposed methodology. Left) Self-supervised pretraining stage where DINOv2 is fine-tuned on the herbicides trials dataset (Section 2.1). Model performance is monitored and optimal weights are selected using the primitives dataset (Section 2.3). Right) Supervised fine-tuning stage where the segmentation model is trained on the BASE dataset (Section 2.2). Model evaluation is performed on the test subset of the BASE dataset (same domain) and two additional datasets to assess domain shift robustness: REALITY CHECK (Section 2.4) and DRONE dataset (Section 2.5).

not released, we initialized them randomly and followed a two-phase training strategy: first training only the heads for 20 epochs, followed by full model training for 1000 epochs.

We evaluated two input resolutions during training: 518x518 pixels, which matches both the default DINOv2 configuration and the resolution of our dataset, and 224x224 pixels, which allowed for a larger global batch size. For the latter, the positional encodings were adapted to the resolution using bicubic interpolation.

Training was performed on 6 NVIDIA Tesla H100 GPUs (80GB each). The global batch size was set to the maximum each GPU could handle without running out of memory: 144 for 518x518 inputs and 360 for 224x224 inputs. The 518x518 resolution matches the original DINOv2 implementation, whereas the 224x224 resolution was selected to enable a batch size closer to the smallest batch size tested in the original implementation (2048) (Oquab et al. (2024)). During head-only training, the base learning rate was set to 2×10^{-3} with 5 warmup epochs. For full model training, the learning rate was reduced to 2×10^{-4} with 10 warmup epochs. All other hyperparameters were kept at their default values.

To monitor learning progress during self-supervised training, model weights were saved every 5 epochs. These checkpoints were evaluated using a linear classification protocol on the primitives dataset (see Section 2.3). The final model weights were selected based on the epoch that achieved the highest classification accuracy, ensuring that the retained foundation model reflects the best representation quality learned during training. Therefore, this stage resulted in two domain-specific models: DINOv2_FT_518 and DINOv2_FT_224, corresponding to the two input resolutions used.

3.2. Supervised fine-tuning

For supervised fine-tuning, we adopted the same architecture and training procedure described in Picon et al. (2025a). The generated domain-specific foundation model was used as the encoder backbone (DINOv2) within a segmentation framework composed of task-specific decoders. The decoder design follows the SegFormer multi-scale architecture (Xie et al. (2021)), allowing efficient integration of features across different spatial scales.

Three independent decoders were used for the tasks of vegetation presence, species identification, and damage classification, as illustrated in Figure 6. The final layer of each decoder was replaced with a 1x1 convolutional layer, with the number of filters corresponding to the number of classes in the task. Softmax activation was used

for multi-class outputs. The encoder weights were frozen during training to preserve the representations learned during the self-supervised pretraining.

Loss functions per task were defined as weighted categorical cross-entropy, with class weights computed using the effective number of samples method (Cui et al. (2019)), extended to semantic segmentation. A beta parameter of 0.99 was used to address class imbalance.

While we followed the same augmentation strategies and optimizer configuration as in Picon et al. (2025a), the dataset split was significantly different. Specifically, training was performed using 80% of the 2019A2 subset and the full 2019A1 subset (373 images), with validation on 10% of 2019A2. The test set remained consistent, using 10% of 2019A2. This change led to a substantial reduction in the amount of labeled data used for training, from 2,393 images in the original setup to just 373, representing an 84.4% decrease.

Training was conducted on an NVIDIA Tesla H100 GPU with 80GB of memory. Considering the size of the input images, the batch size was set to 12.

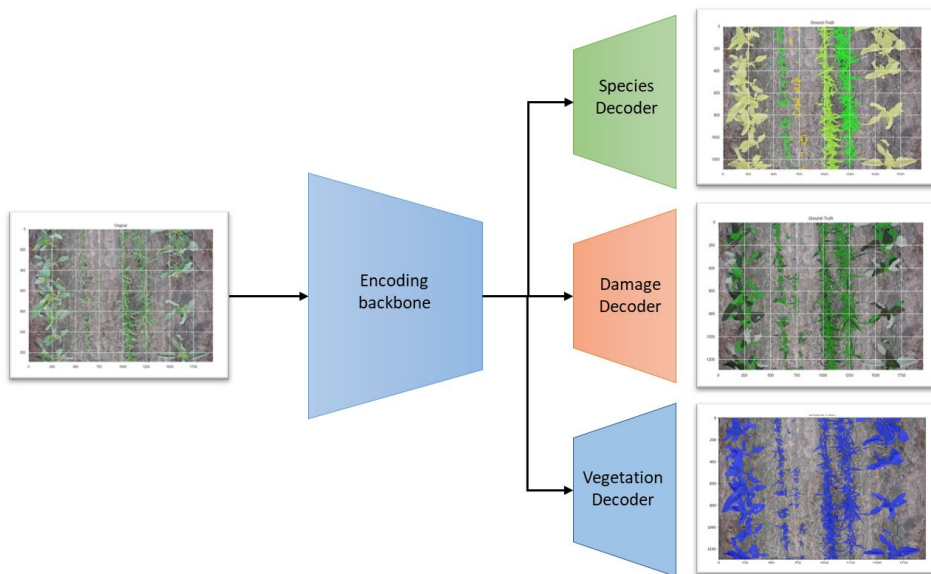


Figure 6: Proposed architecture. An encoding backbone (all the evaluated DINO variants) is connected into three independent decoders. Each decoder covers one of the network tasks (species, damage, and vegetation) (Picon et al. (2025b)).

3.3. Evaluation

To assess the performance and generalization capabilities of the domain-specific foundation model, we conducted a series of experiments focused on semantic segmentation tasks. The evaluation metric used was the F1 score, which balances precision and recall and is well-suited for multi-class segmentation problems with class imbalance.

Evaluation was performed on the BASE test subset and the full REALITY and DRONE datasets, which were not used during training. These datasets encompass diverse acquisition conditions, including variations in camera types, geographic locations, and capture protocols, enabling a robust assessment of domain generalization.

All reported metrics correspond to the best-performing model checkpoint, selected based on the validation performance on the 2019A2 subset.

Moreover, given the importance of accurate species identification in herbicide trials, we conducted detailed analyses for each dataset. This included examining confusion matrices and analyzing the relationship between training data quantity (annotated pixels per class) and model performance.

To further analyze annotation efficiency, we performed an incremental training experiment where the amount of labeled data was progressively reduced. This allowed us to evaluate the model’s performance in low-annotation regimes and its potential to reduce the manual labeling burden. Specifically, we selected an equal number of images from each collection, using increments of 25, 50, 75, 100, and 147 images per collection. This resulted in total training set sizes of 50, 100, 150, 200, and 294 images, respectively. The maximum value of 147 was chosen to match the size of the smallest collection (2019A1), ensuring that the training dataset remains balanced across collections (see Table 1).

Additionally, to gain insight into the learned representations, we visualized the first three principal components of the features extracted by the final block of the transformer encoder. Following the approach of Oquab et al. (2024), Principal Component Analysis (PCA) was applied to reduce the feature dimensionality, and each component was mapped to an RGB channel to generate interpretable visualizations. Background regions were removed using the provided vegetation segmentation masks.

4. Results

In this section, we evaluate the performance of the domain-specific foundation model across multiple semantic segmentation tasks. We report results on datasets with varying acquisition conditions, analyze the impact of reducing labeled data, and visualize the learned representations to better understand the model’s internal features.

4.1. Evaluation on *BASE* and *REALITY* datasets

A comprehensive evaluation of the model was carried out using two distinct datasets to capture both standard performance and generalization under domain shift. The *BASE* dataset (see Section 2.2) served as the foundation for training and initial testing, following the previously described split (see Section 3.2).

To further assess the model’s robustness in more realistic and diverse conditions, we evaluated it using the *REALITY* dataset, which was collected in 2023 across Germany, Spain, and the U.S. Unlike *BASE*, this dataset introduces significant domain shifts. Therefore, by training on *BASE* and testing on *REALITY*, we ensure an unbiased evaluation that reflects the model’s ability to generalize to previously unseen environments and conditions.

Table 5 provides a comparative analysis of the F1 scores achieved by the baseline general-purpose foundation models (DINOv2, DINOv3_web, and DINOv3_sat) and the developed domain-specific variants. While vegetation classification remains consistently high across all models and settings ($F1 = 1.0$), notable improvements are observed in species and damage classification when using domain-specific models.

Specifically, when comparing the best-performing baseline (DINOv2) with the best domain-specific model (DINOv2_FT_224). The F1 score for species classification increased from 0.91 to 0.94 on the *BASE* dataset and from 0.56 to 0.66 on the *REALITY* dataset. For damage classification, the F1 score improved from 0.26 to 0.33 on *BASE* and from 0.17 to 0.27 on *REALITY*.

Figure 7 provides qualitative examples of species identification in the *REALITY* dataset across different model backbones. While all models are capable of accurately detecting vegetation regions, species-level classification remains more challenging. The DINOv2 models consistently yield the best results, with the fine-tuned variants (DINOv2_FT_518 and DINOv2_FT_224) showing slightly improved performance, particularly in identifying less dominant weed species.

Trained/Tested	Encoder/Decoder	F1	F1	F1
		Vegetation	Species	Damage
BASE/BASE	DINOv2/MultiScaleHead	1.0	0.91	0.26
BASE/BASE	DINOv3_web/MultiScaleHead	1.0	0.91	0.15
BASE/BASE	DINOv3_sat/MultiScaleHead	1.0	0.84	0.20
BASE/BASE	DINOv2_FT_518/MultiScaleHead	1.0	0.92	0.32
BASE/BASE	DINOv2_FT_224/MultiScaleHead	1.0	0.94	0.33
BASE/REALITY	DINOv2/MultiScaleHead	1.0	0.56	0.17
BASE/REALITY	DINOv3_web/MultiScaleHead	1.0	0.55	0.11
BASE/REALITY	DINOv3_sat/MultiScaleHead	1.0	0.33	0.11
BASE/REALITY	DINOv2_FT_518/MultiScaleHead	1.0	0.64	0.25
BASE/REALITY	DINOv2_FT_224/MultiScaleHead	1.0	0.66	0.27

Table 5: Metrics of model architectures trained with the BASE dataset (2019) and evaluated against the testing subset of the BASE dataset (2019A2) or the REALITY (2023) dataset.

4.1.1. Species identification

Figure 8 shows the difference between the best performing baseline (DINOv2) and the best domain-specific model (DINOv2_FT_224) tested in the BASE dataset. Overall, the number of misclassifications is reduced in the fine-tuned model, with most predictions remaining unchanged or showing slight improvements. The confusion matrix suggests that DINOv2_FT_224 achieves more consistent accuracy across species, particularly by correcting cases that were previously misclassified by the baseline.

To complement the evaluation on the BASE dataset, Figure 9 presents the confusion matrices obtained from testing in the REALITY dataset. As observed previously, the domain-specific model (DINOv2_FT_224) continues to outperform the baseline (DINOv2), showing stronger diagonal dominance and fewer misclassifications across most categories. Notable improvements are seen in classes such as *porol* (from 0.13 to 0.38) and *solni* (from 0.28 to 0.39), while persistent confusion in *polco* (from 0.09 to 0.13) suggests that certain species remain challenging regardless of training domain.

Furthermore, to understand the effect of the quantity of annotations, a class-wise comparison of F1 score improvements over the best performing general-purpose model (DINOv2) and the best domain-specific model (DINOv2_FT_224) has been performed. As illustrated in Figure 10, the most pronounced improvements are observed in classes with fewer annotated pixels. In contrast, classes with abundant annotations tend to show minimal change, either slight improvements or minimal decreases. This trend is consistent across both the BASE and REALITY evaluations, with improvements being more pronounced in the REALITY dataset. Specifically, *solni* shows the greatest improvement in the BASE evaluation, while *porol* stands out in REALITY.

4.2. Evaluation on the DRONE Dataset: Assessing Domain Shift Robustness

To evaluate how well the model performs under significant domain shifts, we tested it using the DRONE dataset. This dataset differs significantly from the training data in several aspects: the type of image source (drone sensor instead of digital cameras), the time of data collection (2024 vs. 2019), and the surrounding environmental conditions. These differences create a challenging and unbiased scenario to assess the model’s

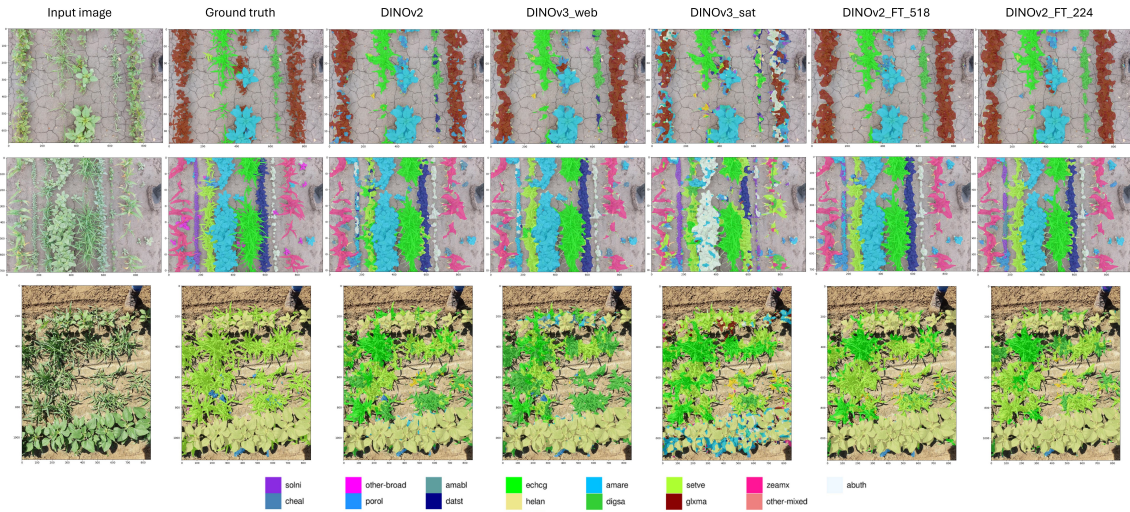


Figure 7: Species predictions generated by each evaluated encoder across different crop fields. Model trained on the BASE dataset and tested on the REALITY dataset: top) *Glycine max* field, middle) *Zea mays* field, bottom) *Helianthus annuus* field.

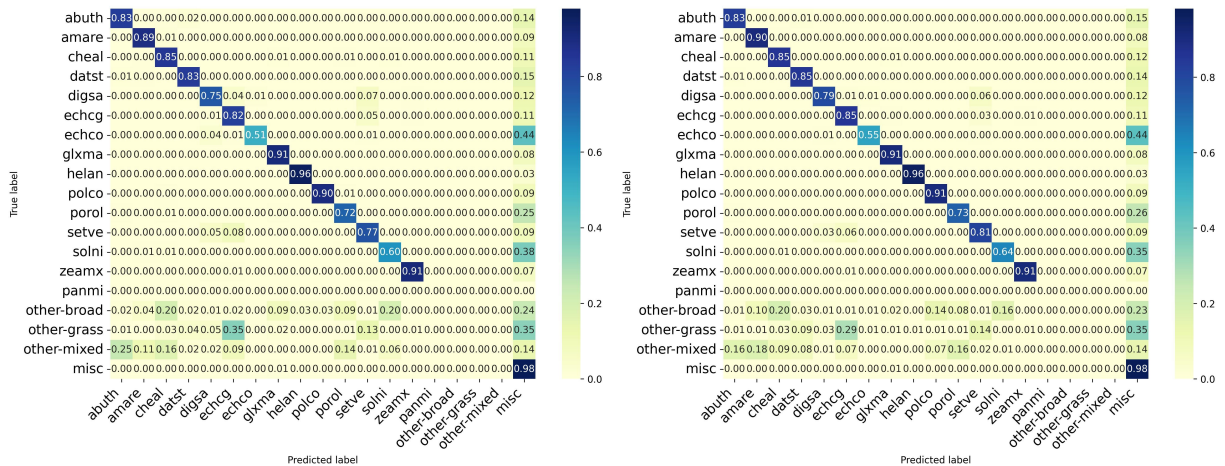


Figure 8: Comparative of the confusion matrices for species identification. Trained and tested on the BASE dataset: left) DINOv2 (Best baseline) right) DINOv2_FT_224 (Best domain-specific foundation model).

ability to generalize. Since manual damage annotations are not available for this dataset, our analysis focuses solely on species identification and vegetation classification.

Table 6 presents a comparative analysis of the F1 scores obtained by the best-performing baseline (DINOv2) and the domain-specific variants on the drones dataset. Despite the challenging conditions, all models maintain perfect F1 scores ($F1 = 1.0$) for vegetation classification.

In contrast, species classification shows clear sensitivity to domain shift. DINOv2 achieves an F1 score of 0.49, while domain-specific fine-tuning leads to consistent improvements, with the best-performing model (DINOv2_FT_224) reaching 0.60.

Examples of species identification in the DRONE dataset are shown in Figure 11. Although all models can accurately detect vegetation areas, distinguishing species is still more difficult. The most notable errors are associated with species labeled as "other", which typically occur when species are either unfamiliar to technicians or not included among the model's supported categories (such as other-grass, other-broad, and other-mixed).

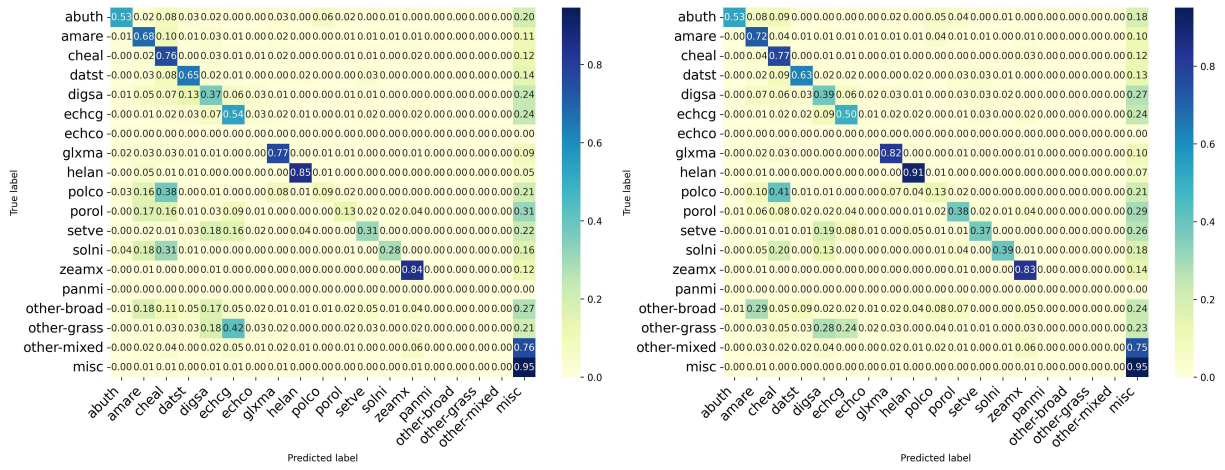


Figure 9: Comparative of the confusion matrices for species identification. Trained on the BASE dataset and tested on the REALITY dataset: left) DINOv2 (Best baseline) right) DINOv2_FT_224 (Best domain-specific foundation model).

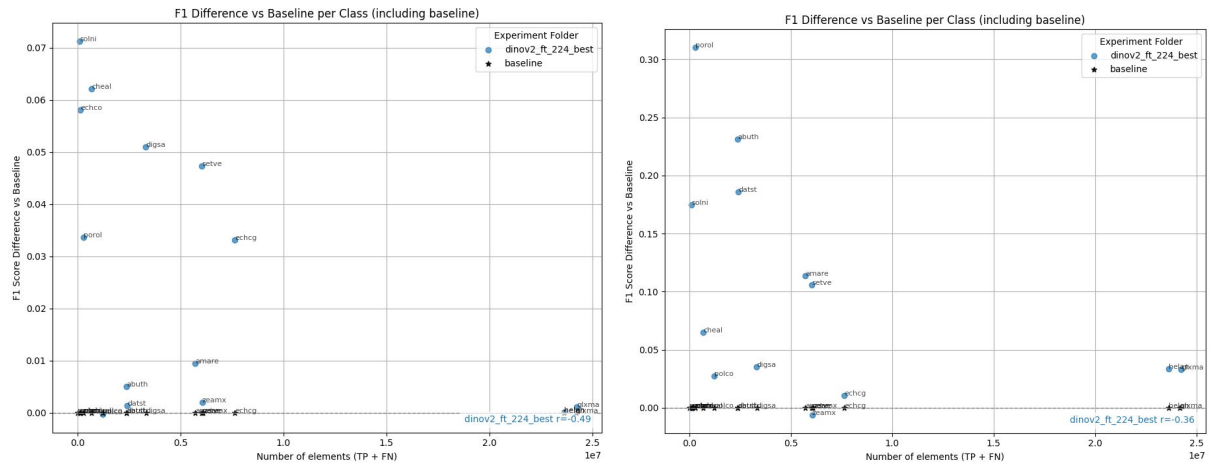


Figure 10: Class-wise comparison of F1 score improvements over the baseline (DINOv2) for species identification. The plot illustrates how model performance varies depending on the number of annotated pixels per class used during training. Trained on the BASE dataset and tested on the : left) BASE dataset, and right) REALITY dataset.

4.2.1. Species identification

Figure 12 compares the top-performing general-purpose model (DINOv2) with the best domain-adapted model (DINOv2_FT_224) on the DRONE dataset. As seen in previous evaluations, the domain-specific model demonstrates a notable reduction in misclassifications across most species. Improvements are particularly evident in categories such as *cheal* and *setve*, while some confusion persists for classes like *solni*, indicating ongoing challenges for certain species.

In addition, Figure 13 explores how the amount of annotated data per class affects model performance on the DRONE dataset. This figure compares the class-wise F1 score improvements achieved by the domain-adapted model (DINOv2_FT_224) over the baseline (DINOv2). The results show that the largest gains are concentrated in species with fewer annotated pixels. In contrast, classes with more extensive annotations tend to exhibit only minor changes, with either slight improvements or negligible declines.

Trained/Tested	Encoder/Decoder	F1	F1
		Vegetation	Species
BASE/DRONE	DINOv2/MultiScaleHead	1.0	0.49
BASE/DRONE	DINOv2_FT_518/MultiScaleHead	1.0	0.54
BASE/DRONE	DINOv2_FT_224/MultiScaleHead	1.0	0.60

Table 6: Performance of models trained on the BASE dataset (2019) and evaluated on the DRONE (2024) dataset.

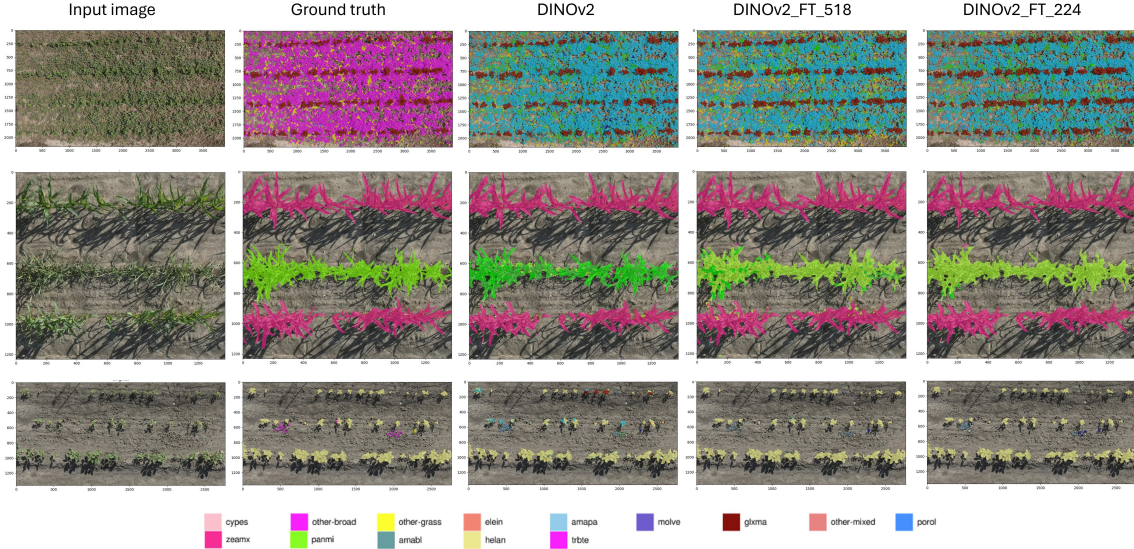


Figure 11: Species predictions generated by each evaluated encoder across different crop fields. Model trained on the BASE dataset and tested on the DRONE dataset: top) *Glycine max* field, middle) *Zea mays* field, bottom) *Helianthus annuus* field.

4.3. Evaluation with Limited Labeled Data

As seen in the previous sections, the domain-specific foundation models show substantial gains in low-data regimes (see Figures 10 and 13). Therefore, to further explore their potential, we evaluate the performance under extremely limited labeled data.

Figure 14 compares the best-performing baseline (DINOv2) and the top domain-specific model (DINOv2_FT_224), each trained on progressively smaller subsets of the BASE dataset. Evaluation is conducted on both the BASE and REALITY datasets to assess generalization across domains.

In the BASE evaluation (left), both models maintain relatively high performance despite the reduced training dataset, with DINOv2_FT_224 consistently outperforming or matching its counterpart across all configurations.

In the REALITY evaluation (right), the advantage of domain-specific pretraining becomes especially pronounced. At every training size, DINOv2_FT_224 consistently outperforms DINOv2, maintaining a clear performance advantage regardless of the amount of labeled data. Notably, with only 25 images per collection (50 total), the domain-specific model achieves an F1 score of 0.59, outperforming both its baseline variant ($F1 = 0.5$) and even the one trained with 147 images per collection (294 total), which only reaches 0.56.

4.4. Visual analysis

Herbicide trial images differ notably from natural ones in their visual properties. They tend to have a more uniform color distribution, and objects in the foreground may not be easily distinguishable due to overlapping

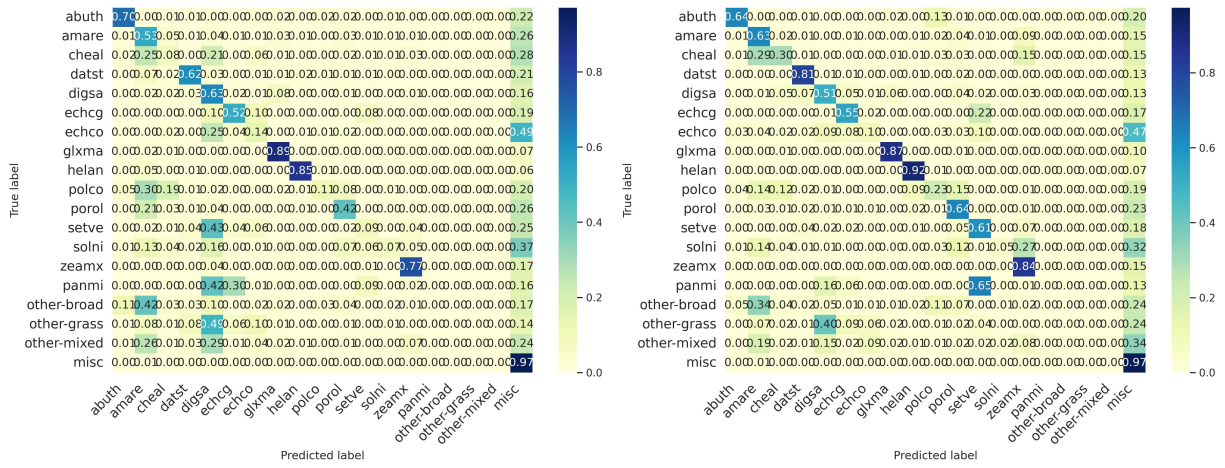


Figure 12: Comparative of the confusion matrices for species identification. Trained on the BASE dataset and tested on the DRONE dataset: left) DINOv2 (Best baseline) right) DINOv2_FT_224 (Best domain-specific foundation model).

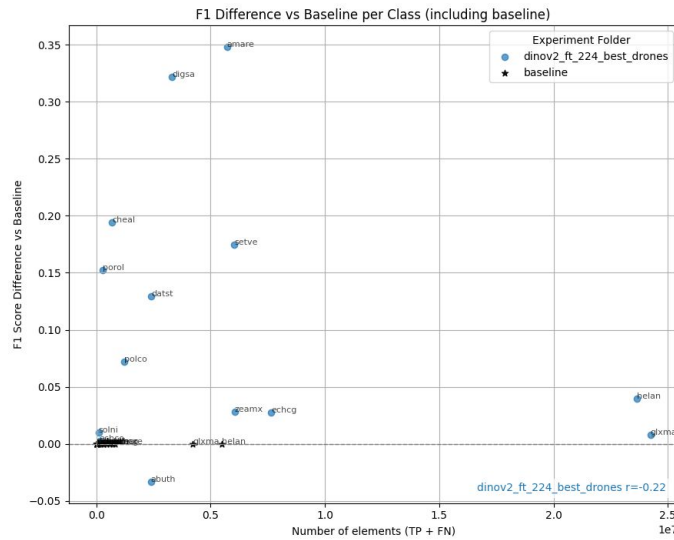


Figure 13: Class-wise comparison of F1 score improvements over the baseline (DINOv2) for species identification. The plot illustrates how model performance varies depending on the number of annotated pixels per class used during training. Trained on the BASE dataset and tested on the DRONE dataset.

elements or background with similar appearances. To separate the background, vegetation segmentation masks provided with the dataset are utilized. For each image whose features are to be visualized, we perform Principal Component Analysis (PCA), and map the first three principal components to the RGB channels to generate the colored visualizations. The same three samples shown in Figure 7 are selected, and their corresponding feature visualizations, extracted by each encoder, are presented in Figure 15.

The visualizations in Figure 15 show that all models effectively capture vegetation structure. DINOv2-based encoders are particularly effective at distinguishing between different species of crops and weeds. The fine-tuned DINOv2 models exhibit improved intra-image consistency, assigning similar colors to plants of the same species within a single image, unlike the non-fine-tuned version, which produces less stable species-level representations.

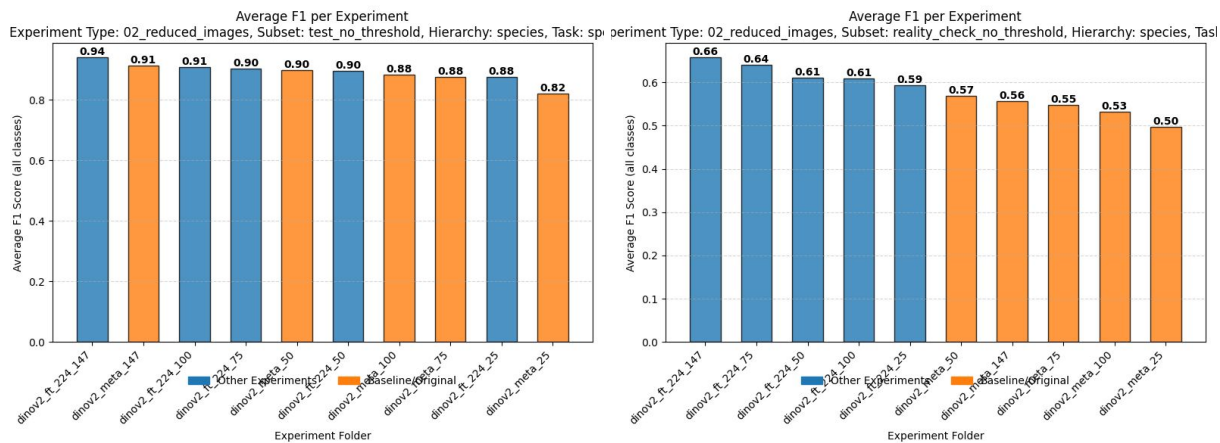


Figure 14: Comparison of F1 score in species identification across models trained with varying amounts of labeled data per collection. The plot illustrates how performance varies depending on the volume of annotated training data. Trained on the BASE dataset and tested on the : left) BASE dataset, and right) REALITY dataset.

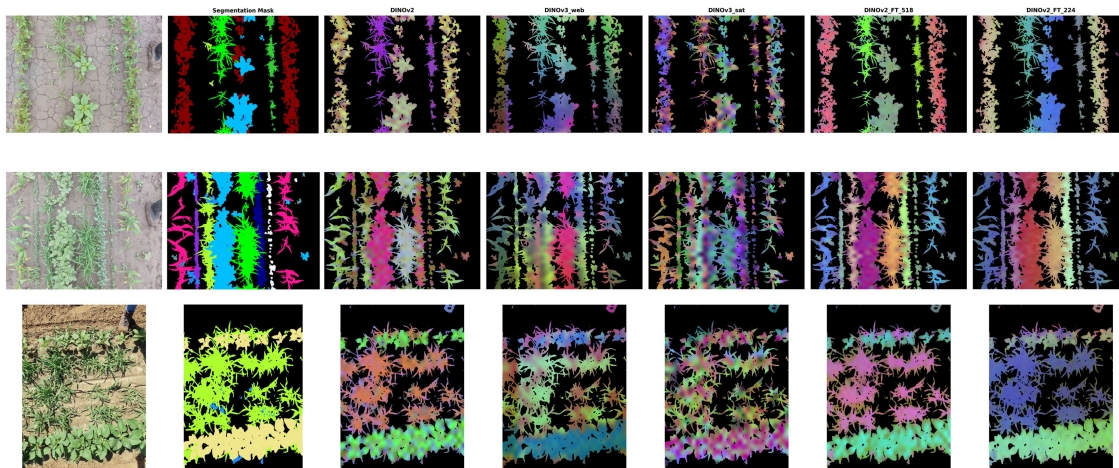


Figure 15: Visualization of the features extracted by each of the evaluated encoders across different crop fields. To generate the colored visualization, PCA is performed on each of the samples, and the first three components are mapped to the RGB channels. The background is removed using the provided vegetation segmentation mask. Features are shown for: top) *Glycine max* field, middle) *Zea mays* field, bottom) *Helianthus annuus* field.

5. Discussion

This study introduces a domain-specific vision foundation model tailored for herbicide trials, trained using a self-supervised learning approach on a large, curated agricultural dataset. The results demonstrate that domain-specific pretraining yields rich and transferable representations, consistently outperforming general-purpose foundation models across semantic segmentation tasks involving multiple plant species and damage types.

On the BASE dataset, which represents low domain shift conditions, the domain-specific model achieves notable improvements in F1 score for both species identification (from 0.91 to 0.94) and damage classification (from 0.26 to 0.33).

These gains are even more pronounced under domain shift scenarios. On the REALITY dataset, which introduces temporal and environmental variability, the model maintains robust performance, with species identification improving from 0.56 to 0.66 and damage classification from 0.17 to 0.27. These results highlight the importance

of domain adaptation. When examining the impact of the backbone on generalization, it becomes evident that general-purpose models suffer more pronounced performance degradation under domain shift, whereas domain-specific models exhibit greater resilience and adaptability to new scenarios.

Moreover, under more extreme domain shifts, including changes in camera types, geographic locations and capture protocols, the model still demonstrates strong generalization, improving species identification F1 score from 0.49 to 0.60. These results further confirm the practical value of domain-specific pretraining. The shift in sensor modality and environmental context introduced by drone data reveals the limitations of general-purpose models and the enhanced adaptability of their domain-specific counterparts.

Given the high cost of manual annotation in agricultural settings, we further examined how the model performs under limited supervision. By progressively reducing the amount of labeled data, we show that the domain-specific model achieves high segmentation accuracy even when data is scarce (see Figure 14). On the REALITY dataset, it achieves a 5.4% higher F1 score than the general-purpose model while requiring 80% fewer labeled samples. These results highlight the annotation efficiency and generalization capacity of domain-specific models, particularly in unseen scenarios. This is particularly relevant in agricultural contexts, where manual annotation is both labor-intensive and costly. The ability to maintain strong performance with limited supervision offers a scalable and cost-effective solution for herbicide trial analysis.

An important methodological consideration in this study was how to optimize pretraining under limited hardware resources. To this end, we trained two versions of the domain-specific model at different input resolutions. This approach enabled a larger global batch size, which is beneficial for self-supervised pretraining (Chen et al. (2020)). Interestingly, the model pretrained at lower resolution (224x224) consistently outperformed the one trained at higher resolution (518x518), despite both surpassing the baseline (see Tables 5 and 6). These results suggest that, within the context of self-supervised pretraining for weed herbicide trials, increasing batch size may have a greater impact on representation quality than input resolution alone.

Despite these optimizations, the overall computational demands of pretraining large vision models remain substantial. Extended training times and the need for high-end hardware can limit the accessibility and scalability of this approach. Future work should explore more resource-efficient training strategies such as Low-Rank Adaptation (LoRA) (Hu et al. (2021)). This approach could be applied to the supervised fine-tuning, where it has already demonstrated strong performance in other downstream tasks (Espejo-Garcia et al. (2025)), or even integrated into the self-supervised pretraining process to enable more accessible and scalable domain adaptation. Additionally, while this study focused on species identification and damage assessment, the proposed approach could be extended to other downstream agricultural tasks, such as disease detection, growth stage estimation, or yield prediction.

6. Conclusions

This research highlights the advantages of domain-specific vision foundation models in agricultural segmentation tasks. While performance differences with general-purpose models are modest under familiar conditions, the benefits become more pronounced in the presence of domain shifts and limited annotation. Through extensive evaluation, we show that domain-specific models consistently outperform their general-purpose counterparts in scenarios that reflect real-world agricultural variability, maintaining strong performance even with reduced supervision.

These findings suggest that domain-specific foundation models are better suited for real-world agricultural scenarios, where variability and limited supervision are common. Additionally, the model’s ability to generalize across datasets and maintain strong performance with fewer annotations supports its potential for scalable deployment.

To fully assess the potential of the domain-specific foundation models, more efficient fine-tuning techniques, such as LoRA, should be explored, to reduce computational costs and improve adaptability. Moreover, expanding the evaluation to a broader range of downstream tasks and datasets would help validate the model’s generalization capabilities and further confirm the advantages of domain-specific foundation models across diverse agricultural scenarios.

Author Contributions

LB-D-V: conceptualization, investigation, software, formal analysis, methodology, and writing -original draft, review and editing. **AP:** conceptualization, investigation, software, formal analysis, methodology, supervision, and writing -review and editing. **DM:** conceptualization, investigation, data curation, software, formal analysis, methodology, and writing -review and editing. **MR:** conceptualization, formal analysis, investigation, methodology, and writing -review and editing. **EP:** conceptualization, investigation, methodology, supervision, and writing -review and editing. **JR:** validation, conceptualization, investigation, and methodology. **CJJ:** validation, methodology, investigation, and conceptualization. **RN-M:** investigation, methodology, and writing -review and editing.

Acknowledgments

All experiments for this work were conducted using Tecnalia’s KATEA computing cluster.

Funding

Some authors have received partial support by the Elkartek Programme, Basque Government (Spain) (DBASKIN (KK-2025/00012))

Declaration of competing interest

LB-D-V, AP and DM were employed by TECNALIA. MR, JR, CJJ, and RN-M were employed by BASF SE.

The remaining authors declare that the research was conducted in the absence of any commercial or financial relationships that could be construed as a potential conflict of interest.

Data availability

The data analyzed in this study is subject to the following licenses/restrictions. The dataset used in this article has been generated by the BASF R&D field research community. It could be made available on reasonable request for non-commercial research purposes and under an agreement with BASF. Requests to access these datasets should be directed to ramon.navarra-mestre@basf.com.

Declaration of Generative AI and AI-assisted technologies in the writing process

During the preparation of this work the authors used ChatGPT and Copilot in order to improve language and readability. After using these tools, the authors reviewed and edited the content as needed and take full responsibility for the content of the publication.

References

- Adhinata, F.D., Wahyono, Sumiharto, R., 2024. A comprehensive survey on weed and crop classification using machine learning and deep learning. *Artificial Intelligence in Agriculture* 13, 45–63. doi:10.1016/j.aiia.2024.06.005.
- Ayllón-Benitez, A., Bernabé-Díaz, J.A., Espinoza-Arias, P., Esnaola-Gonzalez, I., Beeckman, D.S., McCaig, B., Hanzlik, K., Cools, T., Castro Irigorri, C., Palacios, N., 2023. Eppo ontology: a semantic-driven approach for plant and pest codes representation. *Frontiers in Artificial Intelligence* 6, 1131667.
- Bommasani, R., Hudson, D.A., Adeli, E., Altman, R., Arora, S., Arx, S.v., Bernstein, M.S., Bohg, J., Bosselut, A., Brunskill, E., Brynjolfsson, E., Buch, S., Card, D., Castellon, R., Chatterji, N., Chen, A., Creel, K., Davis, J.Q., Demszky, D., Donahue, C., Doumbouya, M., Durmus, E., Ermon, S., Etchemendy, J., Ethayarajh, K., Fei-Fei, L., Finn, C., Gale, T., Gillespie, L., Goel, K., Goodman, N., Grossman, S., Guha, N., Hashimoto, T., Henderson, P., Hewitt, J., Ho, D.E., Hong, J., Hsu, K., Huang, J., Icard, T., Jain, S., Jurafsky, D., Kalluri, P., Karamcheti, S., Keeling, G., Khani, F., Khattab, O., Koh, P.W., Krass, M., Krishna, R., Kuditipudi, R., Kumar, A., Ladhak, F., Lee, M., Lee, T., Leskovec, J., Levent, I., Li, X.L., Li, X., Ma, T., Malik, A., Manning, C.D., Mirchandani, S., Mitchell, E., Munyikwa, Z., Nair, S., Narayan, A., Narayanan, D., Newman, B., Nie, A., Niebles, J.C., Nilforoshan, H., Nyarko, J., Ogut, G., Orr, L., Papadimitriou, I., Park, J.S., Piech, C., Portelance, E., Potts, C., Raghunathan, A., Reich, R., Ren, H., Rong, F., Roohani, Y., Ruiz, C., Ryan, J., Ré, C., Sadigh, D., Sagawa, S., Santhanam, K., Shih, A., Srinivasan, K., Tamkin, A., Taori, R., Thomas, A.W., Tramèr, F., Wang, R.E., Wang, W., Wu, B., Wu, J., Wu, Y., Xie, S.M., Yasunaga, M., You, J., Zaharia, M., Zhang, M., Zhang, T., Zhang, X., Zhang, Y., Zheng, L., Zhou, K., Liang, P., 2022. On the Opportunities and Risks of Foundation Models. doi:10.48550/arXiv.2108.07258.
- Bosilj, P., Aptoula, E., Duckett, T., Cielniak, G., 2020. Transfer learning between crop types for semantic segmentation of crops versus weeds in precision agriculture. *Journal of Field Robotics* 37, 7–19. doi:10.1002/rob.21869.
- Celikkan, E., Saberioon, M., Herold, M., Klein, N., 2023. Semantic Segmentation of Crops and Weeds with Probabilistic Modeling and Uncertainty Quantification, in: 2023 IEEE/CVF International Conference on Computer Vision Workshops (ICCVW), pp. 582–592. doi:10.1109/ICCVW60793.2023.00065. iSSN: 2473-9944.
- Chen, T., Kornblith, S., Norouzi, M., Hinton, G., 2020. A simple framework for contrastive learning of visual representations, in: III, H.D., Singh, A. (Eds.), *Proceedings of the 37th International Conference on Machine Learning*, PMLR. pp. 1597–1607.
- Cui, Y., Jia, M., Lin, T.Y., Song, Y., Belongie, S., 2019. Class-balanced loss based on effective number of samples, in: *Proceedings of the IEEE/CVF Conference on Computer Vision and Pattern Recognition*, pp. 9268–9277.

- Darbyshire, M., Salazar-Gomez, A., Gao, J., Sklar, E.I., Parsons, S., 2023. Towards practical object detection for weed spraying in precision agriculture. *Frontiers in Plant Science* 14. doi:10.3389/fpls.2023.1183277. publisher: Frontiers.
- Dosovitskiy, A., Beyer, L., Kolesnikov, A., Weissenborn, D., Zhai, X., Unterthiner, T., Dehghani, M., Minderer, M., Heigold, G., Gelly, S., Uszkoreit, J., Houlsby, N., 2021. An Image is Worth 16x16 Words: Transformers for Image Recognition at Scale, in: *International Conference on Learning Representations*.
- Dyrmann, M., Mortensen, A.K., Midtiby, H.S., Jørgensen, R.N., 2016. Pixel-wise classification of weeds and crop in images by using a Fully Convolutional neural network. *CIGR-AgEng conference* .
- Espejo-Garcia, B., Güldenring, R., Nalpantidis, L., Fountas, S., 2025. Foundation vision models in agriculture: DINOv2, LoRA and knowledge distillation for disease and weed identification. *Computers and Electronics in Agriculture* 239, 110900. doi:10.1016/j.compag.2025.110900.
- Hu, E.J., Shen, Y., Wallis, P., Allen-Zhu, Z., Li, Y., Wang, S., Wang, L., Chen, W., 2021. LoRA: Low-rank adaptation of large language models, in: *International Conference on Learning Representations*.
- Hu, K., Wang, Z., Coleman, G., Bender, A., Yao, T., Zeng, S., Song, D., Schumann, A., Walsh, M., 2024. Deep learning techniques for in-crop weed recognition in large-scale grain production systems: a review. *Precision Agriculture* 25, 1–29. doi:10.1007/s11119-023-10073-1.
- Juwono, F.H., Wong, W.K., Verma, S., Shekhawat, N., Lease, B.A., Apriono, C., 2023. Machine learning for weed–plant discrimination in agriculture 5.0: An in-depth review. *Artificial Intelligence in Agriculture* 10, 13–25. doi:10.1016/j.aiia.2023.09.002.
- Kumar, S., Kumari, S., Rana, S.S., Rana, R.S., Anwar, T., Qureshi, H., Saleh, M.A., Alamer, K.H., Attia, H., Ercisli, S., Aghayeva, S., 2024. Weed management challenges in modern agriculture: The role of environmental factors and fertilization strategies. *Crop Protection* 185, 106903. doi:10.1016/j.cropro.2024.106903.
- Ma, X., Deng, X., Qi, L., Jiang, Y., Li, H., Wang, Y., Xing, X., 2019. Fully convolutional network for rice seedling and weed image segmentation at the seedling stage in paddy fields. *PLOS ONE* 14, e0215676. doi:10.1371/journal.pone.0215676. publisher: Public Library of Science.
- Milioto, A., Lottes, P., Stachniss, C., 2018. Real-Time Semantic Segmentation of Crop and Weed for Precision Agriculture Robots Leveraging Background Knowledge in CNNs, in: *2018 IEEE International Conference on Robotics and Automation (ICRA)*, pp. 2229–2235. doi:10.1109/ICRA.2018.8460962. iSSN: 2577-087X.
- Mortensen, A.K., Dyrmann, M., Karstoft, H., Jørgensen, R.N., Gislum, R., 2016. Semantic Segmentation of Mixed Crops using Deep Convolutional Neural Network. *CIGR-AgEng conference* .
- Oerke, E.C., 2006. Crop losses to pests. *The Journal of Agricultural Science* 144, 31–43. doi:10.1017/S0021859605005708.
- Oquab, M., Darcet, T., Moutakanni, T., Vo, H., Szafraniec, M., Khalidov, V., Fernandez, P., Haziza, D., Massa, F., El-Nouby, A., Assran, M., Ballas, N., Galuba, W., Howes, R., Huang, P.Y., Li, S.W., Misra, I., Rabbat, M., Sharma, V., Synnaeve, G., Xu, H., Jegou, H., Mairal, J., Labatut, P., Joulin, A., Bojanowski, P., 2024. DINOv2: Learning Robust Visual Features without Supervision. doi:10.48550/arXiv.2304.07193.

- Picon, A., Eguskiza, I., Mugica, D., Romero, J., Jimenez, C.J., White, E., Do-Lago-Junqueira, G., Klukas, C., Navarra-Mestre, R., 2025a. From Field to Drone: Domain Drift Tolerant Automated Multi-Species and Damage Plant Semantic Segmentation for Herbicide Trials. doi:10.48550/arXiv.2508.07514.
- Picon, A., Mugica, D., Eguskiza, I., Bereciartua-Perez, A., Romero, J., Jimenez, C.J., Klukas, C., Gomez-Zamanillo, L., Eggers, T., Navarra-Mestre, R., 2025b. Taxonomic hierarchical loss function for enhanced crop and weed phenotyping in multi-task semantic segmentation. *Smart Agricultural Technology* 10, 100761. doi:10.1016/j.atech.2024.100761.
- Sa, I., Chen, Z., Popović, M., Khanna, R., Liebisch, F., Nieto, J., Siegwart, R., 2018. weedNet: Dense Semantic Weed Classification Using Multispectral Images and MAV for Smart Farming. *IEEE Robotics and Automation Letters* 3, 588–595. doi:10.1109/LRA.2017.2774979.
- Sekachev, B., Manovich, N., Zhiltsov, M., Zhavoronkov, A., Kalinin, D., Hoff, B., TOsmanov, Kruchinin, D., Zankevich, A., DmitriySidnev, Markelov, M., Johannes222, Chenuet, M., a andre, telenachos, Melnikov, A., Kim, J., Ilouz, L., Glazov, N., Priya4607, Tehrani, R., Jeong, S., Skubriev, V., Yonekura, S., vugia truong, zliang7, lizhming, Truong, T., 2020. opencv/cvat: v1.1.0, in: opencv/cvat: v1.1.0, Zenodo. doi:10.5281/zenodo.4009388.
- Siméoni, O., Vo, H.V., Seitzer, M., Baldassarre, F., Oquab, M., Jose, C., Khalidov, V., Szafraniec, M., Yi, S., Ramamonjisoa, M., Massa, F., Haziza, D., Wehrstedt, L., Wang, J., Darcet, T., Moutakanni, T., Sentana, L., Roberts, C., Vedaldi, A., Tolan, J., Brandt, J., Couprie, C., Mairal, J., Jégou, H., Labatut, P., Bojanowski, P., 2025. DINOv3. doi:10.48550/arXiv.2508.10104.
- Xie, E., Wang, W., Yu, Z., Anandkumar, A., Alvarez, J.M., Luo, P., 2021. Segformer: Simple and efficient design for semantic segmentation with transformers. *Advances in neural information processing systems* 34, 12077–12090.